Geophysical Research Letters

RESEARCH LETTER
10.1029/2020GL091034

Key Points:

- Gypsum deltas formed by *outsalting* process due to a mixing between hot saline springs and the Dead Sea's brine
- The gypsum formation ages coincide with times of grand solar minima events, reflecting the sensitivity regional hydrology to global climate

Supporting Information:

- Supporting Information S1

Correspondence to:
N. Weber,
nurit.weber@mail.huji.ac.il

Citation:
Weber, N., Lazar, B., Gavrieli, I., Yechieli, Y., & Stein, M. (2021). Gypsum deltas at the Holocene Dead Sea linked to grand solar minima. *Geophysical Research Letters*, *48*, e2020GL091034. https://doi.org/10.1029/2020GL091034

Received 1 OCT 2020
Accepted 10 FEB 2021

Gypsum Deltas at the Holocene Dead Sea Linked to Grand Solar Minima

N. Weber[1,2], B. Lazar[1], I. Gavrieli[2], Y. Yechieli[2], and M. Stein[1,2]

[1]The Fredy and Nadin Herrman Institute of Earth Sciences, The Hebrew University of Jerusalem, The Edmond J. Safra Campus, Jerusalem, Israel, [2]Geological Survey of Israel, Jerusalem, Israel

Abstract Unique gypsum structures: large capes (termed "*gypsum deltas*") and small pitted gypsum mounds are exposed along the western shores of the currently retreating Dead Sea, the hypersaline terminal lake in the Dead Sea Basin. The *gypsum deltas* were formed during time intervals of low lake stands (~420 ± 10 m below mean sea level), when sulfate-rich Ca chloride brines discharged from the coastal aquifer via saline springs, mixed with the Dead Sea brine and precipitated the gypsum (outsalting process). The ages of formation of the gypsum structures coincide with times of North Atlantic cooling events and grand solar minima suggesting a direct impact of the latter on the Dead Sea hydrology and high sensitivity of the regional hydrology (controlling lake level) to global solar-related events. The temporal occurrence and numbers of the gypsum structures appear to follow the Hallstatt Cycle that approaches minima at ~3,000–2,000 years before present.

Plain Language Summary The man-made retreat of the Dead Sea hypersaline lake exposed unique sedimentary structures with deltaic shape. The structures comprise gypsum minerals that were deposited in the shallow offshore environment of the lake due to mixing of brines discharged by saline springs and the Dead Sea solution. Radiocarbon dating of the gypsum structures indicates that the saline springs discharge (and formation of the structures) coincides with times of North Atlantic cooling events and grand solar minima, a global phenomenon, which appears to impact the regional hydrology. Maximum activity of saline springs discharge and gypsum structure deposition occurred at 3000-2000 years before the present.

1. Introduction

Thick sequences of gypsum, halite, and more soluble salts were deposited in marine environments during about half of earth's history and were typically attributed to evaporative conditions (Cita, 2006; Hsü et al., 1973; Roveri et al., 2014; Warren, 2016 and references therein). Typical evaporitic environments are marine lagoons where excess evaporation (over precipitation) produces saturated brines, which precipitate various evaporite minerals. Water exchange between the lagoon and open-sea maintains a continuous supply of ions for precipitating these evaporite minerals. Non-marine evaporitic gypsum deposits are mainly formed in saline lakes, under excess evaporation conditions (Smoot & Lowenstein, 1991), or as diagenetic precipitation in the sedimentary interstitial space as a result of lake's desiccation (e.g., Mees et al., 2012). Other mechanisms for evaporite rocks formation were also suggested for example, cryogenic salinization, salt focusing, thermal fingering, and hydrothermal outsalting (Craig et al., 1974; Garofalo et al., 2010; Last, 1989; Schoenherr et al., 2009; Starinsky & Katz, 2003). Here, we describe a unique operation mode of the outsalting process that deposited gypsum close to shores of the Dead Sea (Figure 1). The "outsalting" precipitation process is triggered by mixing of two brines with different densities and temperatures, similarly to the formation of salt deposits at the deep bottom of the Red Sea (Hovland et al., 2006, 2015).

We show that during the late Holocene, the outsalting process formed "*gypsum deltas*" and sub-concentric (discordant) gypsum structures (Figure 1b) along the shallow margins of the Dead Sea. The outsalting involved mixing of hot Ca-chloride groundwater with lake's Ca-chloride hypersaline brine when the former discharged at the shore environment. Radiocarbon dating of organic debris in these gypsum structures suggested that sublake groundwater discharge was modulated by solar activity, which has been regarded as a key factor controlling short global climate cycles (e.g., Bond et al., 2001).

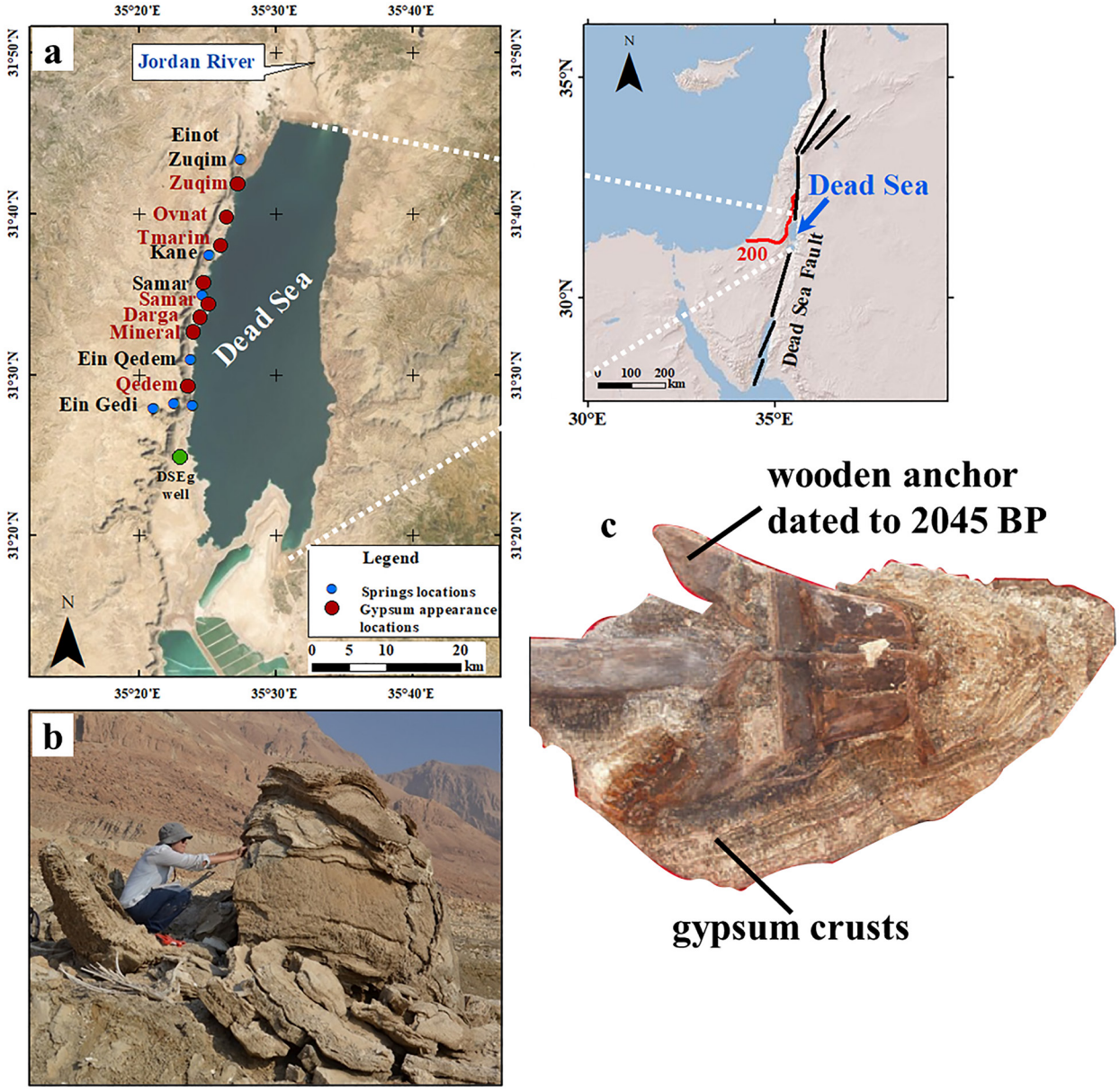

Figure 1. The location and appearance of gypsum structures along the Dead Sea shores: (a) locations of freshwater and saline springs discharge (blue points) along the western shore of the Dead Sea, gypsum structures (red points), and the Ein Gedi (DSEg) drilling site (green). Inset: the Dead Sea Basin located along the Dead Sea Transform Fault (black line), showing the annual 200 mm isopleth (red line), indicating the transition between the Mediterranean and the desert climate zones; (b) isolated gypsum structure at the Ein Qedem shore; (c) Roman anchor that was discovered at the Ein Qedem shore at elevation of 417 m bmsl (below mean sea level). The wooden anchor is coated by gypsum and aragonite crusts (photo from Hadas et al., 2009).

2. Materials and Methods

2.1. Fieldwork

Three cross-sections of the Holocene Ze'elim Formation were measured (Gypsum-1, Gypsum-2, and Gypsum-3; Figure 2a), described and sampled at "Cape Qedem" (landmark of the cliff top 31°29′39.5″N, 35°23′52.9″E). The sections started close to the Qedem drillhole (Figure 2a) drilled ca. 50 m west of the tip of "Cape Qedem" (Stern, 2010). The sections were measured along lines with minimum cover by discordant gypsum structures (two areas surrounded by dashed red lines, Figure 2a) and talus that obscured parts of the stratigraphy along the cliff.

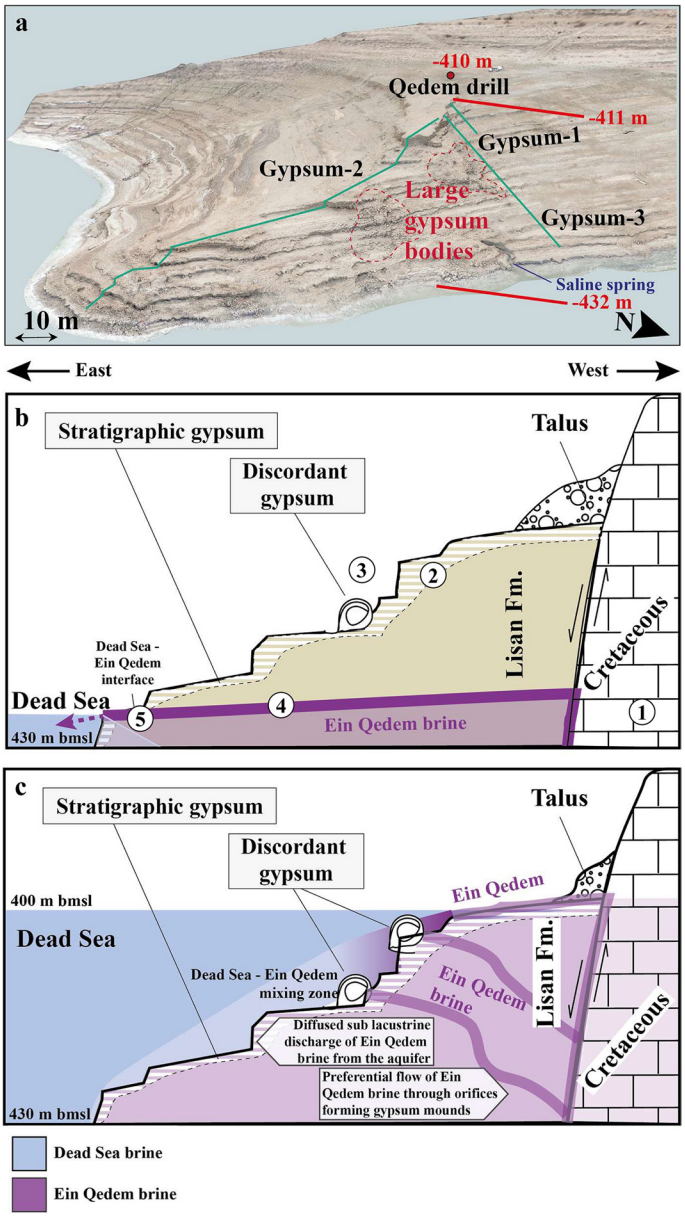

Figure 2. The "*gypsum delta*" of Cape Qedem: (a) an oblique aerial photo of Cape Qedem depicting the sites of the three stratigraphic sections (the green lines) conducted on the cape, cutting through the gypsum delta. The location of Qedem drillhole is marked by the red dot. The photo was taken on January 2020, when lake level was at 434.4 m bmsl. (b) Schematic cross-section along the Gypsum-2 cross section extending from the major fault line in the west to the Dead Sea in the east. The section depicts the: 1. Cretaceous marine carbonate rocks of the Judea Group; 2. The unconformity between the lacustrine sediments of the last Glacial the Lisan Fm. and the overlying gypsum-rich layers of Cape Qedem; 3. Discordant gypsum mounds (Items #2 and #3 are shown also in Figures 3b and 3c); 4. The saline springs that discharge the Ein Qedem brine. The brine rises from a depth of ~1 km depth along the fault plain (thick solid purple line) filling the coastal aquifer (partly transparent purple area) and discharges at the shore; and 5. The interface between the Dead Sea-Ein Qedem brines. (c) Cross-section along the same line as in (b) depicting Cape Qedem during the time of massive gypsum precipitation (e.g. ~3,000–1,000 years BP) when lake level was ~ 30 m higher than at present.

We also describe several discordant gypsum structures in four locations along the Dead Sea shores and an additional gypsum cape at the Tmarim shore (Figure 1a).

2.2. Chronology

Samples of organic debris for radiocarbon dating were collected from "Cape Qedem" stratigraphic sections and from the gypsum structures. Graphitization and radiocarbon measurements were conducted at several Accelerator Mass Spectrometry facilities: the University of Arizona, Australia's Nuclear Science and Technology Organization, National Ocean Sciences Accelerator Mass Spectrometry, Woods Hole, USA, and Poznan Radiocarbon Laboratory, Poland. The radiocarbon measurement uncertainty in all laboratories was smaller than 100 years.

3. Saline Springs and Gypsum Deltas at the Dead Sea Shores

The Ein-Qedem hydrothermal Ca-chloride saline springs (Figures 1a and 2a), with salinity of ~170 g/L (~0.5 the Dead Sea salinity), is the largest brine source discharging to the modern Dead Sea. This type of brine is detected from Einot Zuqim in the north to Hamme Mazor (Ein Gedi-3) in the south (Gavrieli et al., 2001), with the largest flow along the 2 km strip of Qedem shore (Figure 1a). The brine's high temperature (41°–46°C) suggests a rapid ascent from a depth of >950 m (Shalev et al., 2007). The total discharge of the springs is 8–13 MCM/yr (MCM = million cubic meters, Israeli Hydrological Service). The association of the saline springs with prominent gypsum structures, pitted sub-concentric structures and large lakeward pointing triangles, termed here "Capes", for example, "Cape Qedem" (Figure 2a), suggests that during the past several thousand years the geochemical and environmental conditions were favorable for gypsum precipitation.

The geology of Cape Qedem is described by three stratigraphic sections and one borehole (Figures 2a and 3). Section Gypsum-1 (upper 6.5 m of the cape) comprises mainly undulated sequences of detritus, aragonite and gypsum triplets (see Migowski et al., 2006 for this sedimentary facies) and aragonite/gypsum crusts (Figure 3a). Eleven radiocarbon ages, determined on terrestrial organic debris, reveal discontinuous deposition between ~6,600 and ~600 cal yr BP (Figure 3a, Table S1). The sedimentary facies of the section, such as the undulated appearance of the triplets, suggests that its sediments were deposited near shore in shallow waters under waves' activity. During that period, the rather flat top of Cape Qedem comprised a shallow water bank that ended by a steep cliff. A wooden Roman anchor was discovered ~100 m north of the cape's tip at the elevation of 417 m bmsl (Figure 1c) coated by a thick layer of aragonite and gypsum crusts, apparently the mooring location of a boat (Hadas et al., 2009). This top section is rich in aragonite crusts (see also Gypsum-2 and -3; Figure 3a), which formed due to the supply of bicarbonate by freshwater (Belmaker et al., 2019; Bookman et al., 2004; Kagan et al., 2015).

The great abundance of gypsum in sections Gypsum-1, -2, and -3 is unique to Cape Qedem area (Figure 3). Outcrops to the north and south of these three sections (Figure S1), show typical sedimentary facies of the contemporaneous late Holocene Ze'elim Fm. (e.g., Zeelim Gully, Bookman et al., 2004), or the section comprising the Ein Gedi core (Migowski et al., 2006; Figure 3a). Apparently, the gypsum rich central part of Cape Qedem, *interfingers* with the adjacent "typical" sections of the Holocene Ze'elim Fm. Moreover, the gypsum sequences lie unconformably on erosional relief of the last glacial Lisan Fm. (Figures 2b, 3, and S1), as indicated by the ~24 ka age that was measured ~7 m below the top of the Cape at the Qedem drill (Figure 3a). Gypsum structures (discordant gypsum bodies in Figures 3b and 3c) of late Holocene ages (~3,000–~1,000 cal yr BP) lie unconformably on the relief formed by the Holocene gypsum (stratigraphic gypsum in Figures 3b and c). The geometric shape of Cape Qedem resembles that of conventional fan-shaped alluvial deltas at their mouth. However, unlike an alluvial delta, the unique setting of the Qedem "*gypsum delta*" was formed by chemical precipitation in the place where subsurface diffused discharge of the Ein Qedem brine mixed with Dead Sea brines (*gypsum outsalting*) in very shallow water close to the lake's shore (Figure 2c). The mixing of the brines initiated gypsum precipitation due to supersaturation and gypsum nucleation and was maintained by further growth of gypsum crystals. Formation of impressive gypsum structures as a result of mixing between two solutions is also known from other locations worldwide, for example, the Naica Mine, Mexico, the location of world's largest gypsum crystals. These gigantic crystals

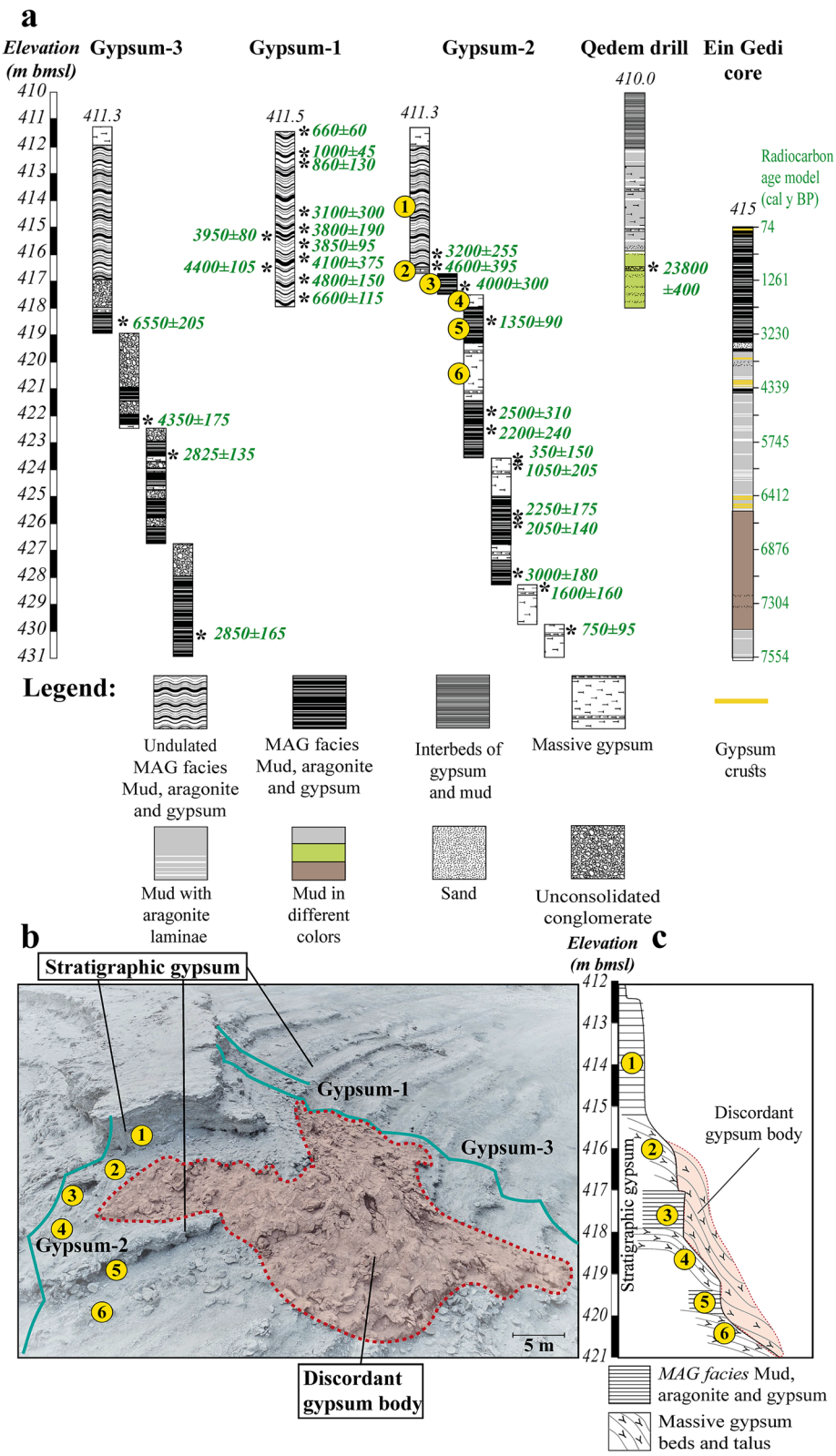
a
Elevation (m bmsl)
Gypsum-3
Gypsum-1
Gypsum-2
Qedem drill
Ein Gedi core
Radiocarbon age model (cal y BP)
410
411
412
413
414
415
416
417
418
419
420
421
422
423
424
425
426
427
428
429
430
431
411.3
411.5
411.3
410.0
415
74
1261
3230
4339
5745
6412
6876
7304
7554
660±60
1000±45
860±130
3100±300
3800±190
3950±80
3850±95
4100±375
4400±105
4800±150
6600±115
3200±255
4600±395
4000±300
1350±90
2500±310
2200±240
350±150
1050±205
2250±175
2050±140
3000±180
1600±160
750±95
6550±205
4350±175
2825±135
2850±165
23800 ±400
Legend:
Undulated MAG facies Mud, aragonite and gypsum
MAG facies Mud, aragonite and gypsum
Interbeds of gypsum and mud
Massive gypsum
Gypsum crusts
Mud with aragonite laminae
Mud in different colors
Sand
Unconsolidated conglomerate
b
Stratigraphic gypsum
Gypsum-1
Gypsum-3
Gypsum-2
5 m
Discordant gypsum body
c
Elevation (m bmsl)
412
413
414
415
416
417
418
419
420
421
Stratigraphic gypsum
Discordant gypsum body
MAG facies Mud, aragonite and gypsum
Massive gypsum beds and talus

were precipitated by mixing of shallow saline waters of evaporative origin, with the regional deep phreatic fluids (Garofalo et al., 2010).

At the Dead Sea shore, the hard gypsum structures are more resistant to erosion than the contemporaneous unconsolidated lacustrine sediments of Holocene Dead Sea (the Zeelim Fm.), and their ubiquitous appearance along the shores indicate that at that period, the saline springs activity was highly enhanced compared to present.

4. Sub-Concentric Mound-Like "Gypsum Structures" Along the Dead Sea Shores

Numerous small (human-size) mound-like sub-concentric discordant "gypsum structures" (e.g., Figure 1b) are pitted along the retreating western shores of the Dead Sea, typically at the elevation of ~420–430 m bmsl (Figures 1a and 4). They vary in diameter between a few tens of centimeters to several meters and comprise layers of bladed gypsum crystals, few centimeters in length and thin crusts of soft gypsum and aragonite. This facies is very similar to the discordant gypsum body in Cape Qedem (Figures 2a, 3b and 3c) and the thick gypsum layers in Cape Qedem outcrop. Many of these structures appear to grow around a wood or boulder. In a unique case, a wooden anchor of a Roman boat (Figure 1c) dated to 2,045 ± 45 cal yr BP (Hadas et al., 2009) was found encrusted with concentric massive gypsum, very close to the location of Gypsum-3 section (Figure 2a). Many sub-concentric gypsum structures and a large "gypsum Cape" structure are exposed at the Tmarim shore (Figure 1a). Presumably, these are sites of local outsalting triggered by mixing of sulfate-rich Ca-chloride brines of the Ein Qedem type, that discharged through small orifices on the nearshore bottom of the lake and mixed with Dead Sea brine (Figure 2c). The outsalting mechanism proposed here can explain similar appearances of gypsum structures in other saline lake environments, for example, the saline springs zone on the south-western marginal zone of Danakil depression Ethiopia (See Figures 1.40 and 11.17 in Warren, 2016).

All the gypsum mound structures that are exposed at the Dead Sea shores at elevation of 420–430 m bmsl were formed between ~4,000 and ~600 cal yr BP (Table S2). However, most of the ages determined on random samples taken from these structures lie between 3,000–1,000 cal yr BP, contemporaneous with the ages of the "stratigraphic gypsum" (Figures 2a and 3) comprising the *gypsum delta* at Cape-Qedem. The chemical properties of brines and sediments, the textures, and structures of the gypsum minerals (e.g., the undulating gypsum in the upper part of Gypsum-1 section) and the structure of Cape Qedem (Figures 2a and 3) suggest that the Qedem-type gypsum was deposited in places of hot-saline groundwater emergence. The modern and historical record show that such springs are active close to the shore; therefore, our interpretation is that the gypsum deposited in conditions of very shallow waters when the lake was at a lowstand around the elevation of 420 m bmsl.

5. Periods of Saline Springs Activity

The drying of the Southern Levant during the post glacial-early Holocene periods is reflected by a significant lake level drop, from ~200 m bmsl at ~14,000 cal yr BP to ~400 m bmsl at the early Holocene (Figure 4; e.g., Stein et al., 2010). During the last glacial Marine Isotop Stage 2 period (~30,000–14,000 cal yr BP) when Lake Lisan was at its highest stands, waters from its relatively low salinity epilimnion (~0.5 the modern Dead Sea salinity) infiltrated the marginal aquifers of the lake; at lake's lowstand, these waters (modified slightly by water/rock interaction) returned back to the Dead Sea as series of saline springs of the Ein Qedem type (Weber et al., 2018). Most of the current saline springs' activity is located along a narrow shore

Figure 3. (a) Stratigraphic sections at Cape Qedem and Ein Gedi spa (see locations in Figures 1a and 2a). Radiocarbon dated samples (Table S1) are marked by the asterisks and the ages are reported as cal yr BP (years before 1950). Sections Gypsum-2 and Gypsum-3 are fragmented to structural steps in the field (see also item (c) below) in which ages are ordered according to the law of superposition. The unconsolidated conglomerate comprises talus of gypsum fragments that were formed at the lake's shores by waves erosion. The Ein Gedi core was described and radiocarbon dated by Migowski et al., (2006); (b) drone's photo of the top of Cape Qedem (Figure 2a) showing the upper location of the sections and the exposure of the gypsum discordant body between sections Gypsum-2 and -3; (c) geological section of the upper 9 m at Cape Qedem showing the field relation between the stratified units and the gypsum discordant body. The circled numbers with yellow background mark the locations of the same rock units in (a), (b), and (c).

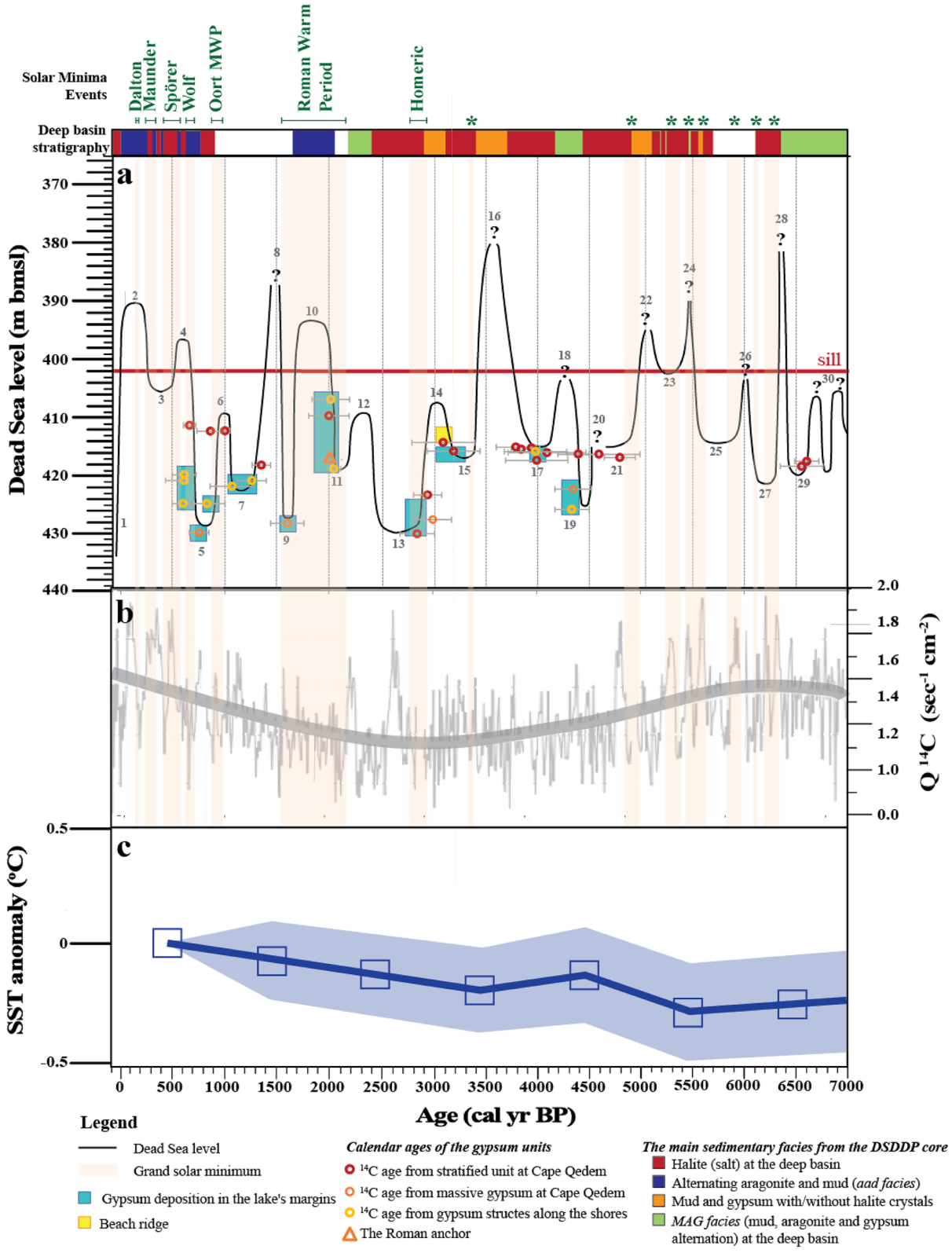
Solar Minima Events
Dalton Minimum
Spörer
Wolf
Oort MWP
Roman Warm Period
Homeric
Deep basin stratigraphy
a
b
c
Dead Sea level (m bmsl)
sill
Q ¹⁴C (sec⁻¹ cm⁻²)
SST anomaly (°C)
Age (cal yr BP)
Legend
Dead Sea level
Grand solar minimum
Gypsum deposition in the lake's margins
Beach ridge
Calendar ages of the gypsum units
¹⁴C age from stratified unit at Cape Qedem
¹⁴C age from massive gypsum at Cape Qedem
¹⁴C age from gypsum structes along the shores
The Roman anchor
The main sedimentary facies from the DSDDP core
Halite (salt) at the deep basin
Alternating aragonite and mud (aad facies)
Mud and gypsum with/without halite crystals
MAG facies (mud, aragonite and gypsum alternation) at the deep basin

strip between Mineral Beach to Ein Gedi (Figure 1a), while the brackish water of Einot Zuqim in the northern part of the Dead Sea is a mixture of the Ein Qedem brine and freshwater. The widespread distribution of these late Holocene gypsum bodies indicates that during that period, the saline springs were much more active and widespread, reaching as far north as Einot Zuqim (Figure 1a).

Several lines of evidence indicate that the isolated gypsum mounds were formed close to the lake surface (most of them found at ~420–430 m bmsl); for example, the location of modern saline springs discharge at or just below the shoreline, and the appearance of aragonite crusts that require bicarbonate supply (from freshwater) at the shore environment (e.g., Bookman et al., 2004). Thus, the isolated gypsum structures are used here as lake level markers for refining the details of the lake level curve for the last 7,000 years (Figure 4). The interpretation of their being low level markers is consistent with the contemporaneous deposition of salt in the deepest floor of the Dead Sea as discovered by the International Continental Scientific Drilling Program drilling (see Kiro et al., 2016, 2017 and Figure 4). Apparently, during most of the Holocene the lake was at low stands (Figure 4), significantly below ~402 m bmsl, the elevation of the sill that separates topographically between the southern very shallow basin of the Dead Sea from the deep northern basin.

The saline springs were mainly active in the latter part of the arid interval, prior to the restoration of freshwater supply from the Judea Mountains aquifers to the Dead Sea that led the deposition of the aragonite crusts. For example, we describe the sequence of events between ~3,600 to 3,000 cal yr BP (Figure 4): (1) at ~3,400 cal yr BP the lake dropped from its high late Bronze period stand; at the same time (2) salt was deposited at the deep basin of the lake; followed by (3) formation of gypsum deltas and gypsum structures at the Dead Sea shore; followed by (4) deposition of aragonite crusts (see the different colored areas in Figure 4). Item #14 marks the renewal of freshwater-springs activity (Kagan et al., 2015).

6. Gypsum Structures Formation and Relation to Grand Solar Minima Events

The gypsum structures were formed at the Dead Sea shores during periods of low lake stands and as suggested above, in association with enhanced discharge of the saline springs (Figures 2c and 4). The low lake stands reflect periods of enhanced aridity in the lake's watershed that in turn were controlled by "global climate impactors." Kushnir and Stein (2019) examined in details the hydroclimate conditions in the Levant and Nile-land regions during the Medieval Warm Period that corresponds to the time interval of ~950–1,100 years AD. They argued that the period of aridity in the Levant and Nile-land coincides with the time of the Oort grand solar minimum. The Oort minimum is linked with intensified El Niño activity, which is known to suppress the African summer monsoon rains in the Ethiopian Highlands. It appears that all intervals of low Dead Sea stand and gypsum structure formation at the near-shores and salt deposition in the deep lake coincide with cold events in the North Atlantic and with solar minima (the pink intervals at Figure 4). Bond et al. (2001) argued that solar activity modulated the cold events in the North Atlantic that in turn affected regional hydrology worldwide. Additionally, the temporal distribution and number of occurrences of the gypsum structures appear to match the ^{10}Be and ^{14}C oscillation that was termed as the *Hallstatt* cycle (e.g., Figure 4b). This oscillation was found in paleoclimate records throughout the Holocene and suggested to be coherent to the major stable resonance of the four Jovian planets (Scafetta et al., 2016).

Recently, Bova et al. (2021) suggested that the climate has been warming since the early Holocene and the global mean annual temperatures increased in temperatures over the past 6,500 years due to rise in the

Figure 4. (a) New reconstruction of the Dead Sea level curve of the past 7,000 years, the Mid to late Holocene (black line; compilation based on data from Bartov et al., 2004; Bookman et al., 2004; Kagan et al., 2015; Kushnir & Stein, 2019; Migowski et al., 2006; Stern, 2010; and the current study). The red line (at 402 m bmsl) marks the elevation of the sill separating between the southern (shallow) and northern (deep) basins of the lake. The main sedimentary facies at the deep basin marked in the upper panel (data from the Dead Sea Deep Drilling Project core, Goldstein et al., 2020; Kiro et al., 2016). Circles mark calendar ages (from radiocarbon dating) of the gypsum units: stratified gypsum unit of "Cape Qedem" (red), the discordant gypsum structures at "Cape Qedem" (orange), the location of gypsum structures from various sites along the Dead Sea shore (yellow), and the Roman anchor marked by orange triangle (ages in Tables S1 and S2). The blue bands delineate periods and elevations of gypsum deposition on the lake's margins. Yellow square indicates the elevation and age of the beach ridge at Ze'elim gully that comprises aragonite crusts. The green intervals and names (green asterisks for no available name) at the top are the grand solar minima (Usoskin et al., 2016). Numbers 1–30 above the high/low stands are listed in Table S3, which presents the sources of data used for the reconstructing the lake level curve. (b) The gray curve is an average of the radiocarbon global production rate showing minimum values between ~3,000 and 1,500 cal yr BP (Usoskin et al., 2016). The data illustrate the "*Hallstatt* cycle" that possibly reflects solar effects on the earth regional climates. (c) Mean annual sea surface temperature anomaly reconstruction with the uncertainties shaded (Bova et al., 2021).

greenhouse gas concentrations (Figure 4c). The minima of Dead Sea surface level decreased during this period, punctuated by several short level rises (Figure 4a). This apparent correlation attests to the response of the Dead Sea hydrological system to global climate drivers.

The activity of the hydrological system in the Dead Sea region is extremely sensitive to the hydroclimate conditions induced by the natural variations in solar irradiance. The new reconstructed lake level curve and the sequences of appearance of salt-gypsum-aragonite crusts in the geological sections reveal a complicated response of the regional hydrological system to the "global climate impactors." Thus, our study clearly demonstrates the sensitivity of the regional hydro-climate regime to changes in external radiative forcing. In a broader view, the Dead Sea surface lies at very low elevation during most of the Holocene indicating on a persistent regional aridity in the East Mediterranean-Levant during this period.

7. Conclusions

Gypsum deltas and pitted gypsum structures are scattered along the western shores of the Dead Sea at elevations of ~420–430 m bmsl, possibly representing sites of former saline springs discharge to the shallow-water shore environment of the late Holocene Dead Sea.

Mixing of Ein Qedem type brine with the Dead Sea brine, caused gypsum outsalting and formation of the pitted gypsum and large *gypsum deltas* (e.g., "Cape Qedem") that spreads over the relief of the last glacial Lisan Formation.

The ages of formation of the *gypsum deltas* and pitted gypsum structures, during low lake levels (and halite deposition in the deep basin), coincide with timings of grand solar minima.

During most of the Holocene, the Dead Sea was at low level, below the sill that separates between the northern and southern basins of the lake. This configuration indicates lasting and persistent aridity in the East Mediterranean-Levant region during most of this period.

Data Availability Statement

Data are available in the supporting information and in Mendeley Data website: http://dx.doi.org/10.17632/467ggzd7ph.2.

Acknowledgments
This work was supported by the Israeli government under GSI DS project 40573, the PALEX project funded by the DFG, Germany (Grant No. BR2208/13-1/-2 to B. Lazar and M. Stein) and the Dead Sea Excellence Center of the Israel Science Foundation (Grant No. 1736/11 to B. Lazar and M. Stein).

References

Bartov, Y. (2004). *Sedimentary fill analysis of a continental basin: The late Pleistocene Dead Sea* (PhD thesis). The Hebrew University of Jerusalem.

Belmaker, R., Lazar, B., Stein, M., Taha, N., & Bookman, R. (2019). Constraints on aragonite precipitation in the Dead Sea from geochemical measurements of flood plumes. *Quaternary Science Reviews*, *221*, 105876. https://doi.org/10.1016/j.quascirev.2019.105876

Bond, G., Kromer, B., Beer, J., Muscheler, R., Evans, M. N., Showers, W., et al. (2001). Persistent solar influence on North Atlantic climate during the Holocene. *Science*, *294*(5549), 2130–2136. https://doi.org/10.1126/science.1065680

Bookman, R., Enzel, Y., Agnon, A., & Stein, M. (2004). Late Holocene lake levels of the Dead Sea. *Bulletin of the Geological Society of America*, *116*(5–6), 555–571. https://doi.org/10.1130/B25286.1

Bova, S., Rosenthal, Y., Liu, Z., Godad, S. P., & Yan, M. (2021). Seasonal origin of the thermal maxima at the Holocene and the last interglacial. *Nature*, *589*(7843), 548–553. https://doi.org/10.1038/s41586-020-03155-x

Cita, M. B. (2006). Exhumation of Messinian evaporites in the deep-sea and creation of deep anoxic brine-filled collapsed basins. *Sedimentary Geology*, *188–189*, 357–378. https://doi.org/10.1016/j.sedgeo.2006.03.013

Craig, J. R., Fortner, R. D., & Weand, B. L. (1974). Halite and hydrohalite from Lake Bonney, Taylor Valley, Antarctica. *Geology*, *2*(8), 389–390.

Garofalo, P. S., Fricker, M. B., Günther, D., Forti, P., Mercuri, A. M., Loreti, M., & Capaccioni, B. (2010). Climatic control on the growth of gigantic gypsum crystals within hypogenic caves (Naica mine, Mexico)? *Earth and Planetary Science Letters*, *289*(3–4), 560–569. https://doi.org/10.1016/j.epsl.2009.11.057

Gavrieli, I., Yechieli, Y., Halicz, L., Spiro, B., Bein, A., & Efron, D. (2001). The sulfur system in anoxic subsurface brines and its implication in brine evolutionary pathways: The Ca-chloride brines in the Dead Sea area. *Earth and Planetary Science Letters*, *186*(2), 199–213. https://doi.org/10.1016/S0012-821X(01)00247-3

Goldstein, S. L., Kiro, Y., Torfstein, A., Kitagawa, H., Tierney, J. E., & Stein, M. (2020). Revised chronology of the ICDP Dead Sea deep drill core relates drier-wetter-drier climate cycles to insolation over the past 220 kyr. *Quaternary Science Reviews*, *244*(15), 106460. https://doi.org/10.1016/j.quascirev.2020.106460

Hadas, G., Segal, I., Yoffe, O., & Stein, M. (2009). Study of roman anchor from the Dead Sea Shore. *Archaeometry*, *51*(6), 1008–1014. https://doi.org/10.1111/j.1475-4754.2009.00462.x

Hovland, M., Kuznetsova, T., Rueslåtten, H., Kvamme, B., Johnsen, H. K., Fladmark, G. E., & Hebach, A. (2006). Sub-surface precipitation of salts in supercritical seawater. *Basin Research*, *18*(2), 221–230. https://doi.org/10.1111/j.1365-2117.2006.00290.x

Hovland, M., Rueslåtten, H., & Johnsen, H. K. (2015). Red Sea salt formations—A result of hydrothermal processes. In N. M. A. Rasul & I. C. F. Stewart (Eds.), *The Red Sea - The Formation, Morphology, Oceanography and Environment of a Young Ocean Basin* (pp. 187–203). Berlin: Springer. https://doi.org/10.1007/978-3-662-45201-1_11

Hsü, K. J., Ryan, W. B. F., & Cita, M. B. (1973). Late Miocene desiccation of the Mediterranean. *Nature*, *242*(5395), 240–244. https://doi.org/10.1038/242240a0

Kagan, E. J., Langgut, D., Boaretto, E., Neumann, F. H., & Stein, M. (2015). Dead Sea levels during the bronze and iron ages. *Radiocarbon*, *57*(2), 237–252. https://doi.org/10.2458/azu

Kiro, Y., Goldstein, S. L., Garcia-Veigas, J., Levy, E., Kushnir, Y., Stein, M., & Lazar, B. (2017). Relationships between lake-level changes and water and salt budgets in the Dead Sea during extreme aridities in the Eastern Mediterranean. *Earth and Planetary Science Letters*, *464*, 211–226. https://doi.org/10.1016/j.epsl.2017.01.043

Kiro, Y., Goldstein, S. L., Lazar, B., & Stein, M. (2016). Environmental implications of salt facies in the Dead Sea. *The Geological Society of America Bulletin*, *128*(5–6), 824–841. https://doi.org/10.1130/b31357.1

Kushnir, Y., & Stein, M. (2019). Medieval climate in the Eastern Mediterranean: Instability and evidence of solar forcing. *Atmosphere*, *10*(1), 1–26. https://doi.org/10.3390/atmos10010029

Last, W. M. (1989). Continental brines and evaporites of the northern Great Plains of Canada. *Sedimentary Geology*, *64*, 207–221.

Mees, F., Casteneda, C., Herrero, J., & van Ranst, E. (2012). The nature and significance of variations in gypsum crystal morphology in Dry Lake Basins. *Journal of Sedimentary Research*, *82*(1), 37–52. https://doi.org/10.2110/jsr.2012.3

Migowski, C., Stein, M., Prasad, S., Negendank, J. F. W., & Agnon, A. (2006). Holocene climate variability and cultural evolution in the Near East from the Dead Sea sedimentary record. *Quaternary Research*, *66*(3), 421–431. https://doi.org/10.1016/j.yqres.2006.06.010

Roveri, M., Flecker, R., Krijgsman, W., Lofi, J., Lugli, S., Manzi, V., et al. (2014). The Messinian Salinity Crisis: Past and future of a great challenge for marine sciences. *Marine Geology*, *352*, 25–58. https://doi.org/10.1016/j.margeo.2014.02.002

Scafetta, N., Milani, F., Bianchini, A., & Ortolani, S. (2016). On the astronomical origin of the Hallstatt oscillation found in radiocarbon and climate records throughout the Holocene. *Earth-Science Reviews*, *162*, 24–43. https://doi.org/10.1016/j.earscirev.2016.09.004

Schoenherr, J., Reuning, L., Kukla, P. A., Littke, R., Urai, J. L., Siemann, M., & Rawahi, Z. (2009). Halite cementation and carbonate diagenesis of intra-salt reservoirs from the Late Neoproterozoic to Early Cambrian Ara Group (South Oman Salt Basin). *Sedimentology*, *56*(2), 567–589. https://doi.org/10.1111/j.1365-3091.2008.00986.x

Shalev, E., Lyakhovsky, V., & Yechieli, Y. (2007). Is advective heat transport significant at the Dead Sea basin? *Geofluids*, *7*(3), 292–300. https://doi.org/10.1111/j.1468-8123.2007.00190.x

Smoot, J. P., & Lowenstein, T. K. (1991). Chapter 3 Depositional environments of non-marine evaporites. *Developments in Sedimentology*, *50*(C), 189–347. https://doi.org/10.1016/S0070-4571(08)70261-9

Starinsky, A., & Katz, A. (2003). The formation of natural cryogenic brines. *Geochimica et Cosmochimica Acta*, *67*(8), 1475–1484. https://doi.org/10.1016/S0016-7037(02)01295-4

Stein, M., Torfstein, A., Gavrieli, I., & Yechieli, Y. (2010). Abrupt aridities and salt deposition in the post-glacial Dead Sea and their North Atlantic connection. *Quaternary Science Reviews*, *29*(3–4), 567–575. https://doi.org/10.1016/j.quascirev.2009.10.015

Stern, O. (2010). *Geochemistry, hydrology and paleo-hydrology of Ein Qedem spring system (MSc thesis)*. Jerusalem: Hebrew University of Jerusalem.

Usoskin, I. G., Gallet, Y., Lopes, F., Kovaltsov, G. A., & Hulot, G. (2016). Solar activity during the Holocene: The Hallstatt cycle. *Astronomy & Astrophysics*, *587*(A150), 1–10. https://doi.org/10.1051/0004-6361/201527295

Warren, J. K. (2016). *Evaporites: A geological compendium*. (2nd ed., pp. 1–1813). New York, NY: Springer. https://doi.org/10.1007/978-3-319-13512-0

Weber, N., Yechieli, Y., Stein, M., Yokochi, R., Gavrieli, I., Zappala, J., et al. (2018). The circulation of the Dead Sea brine in the regional aquifer. *Earth and Planetary Science Letters*, *493*, 242–261. https://doi.org/10.1016/j.epsl.2018.04.027